Journal of Solid State Chemistry 184 (2011) 1333–1338

Contents lists available at ScienceDirect

Journal of Solid State Chemistry

journal homepage: www.elsevier.com/locate/jssc

Fabrication of TiN nanorods by electrospinning and their electrochemical properties

Dongfei Sun, Junwei Lang, Xingbin Yan*, Litian Hu, Qunji Xue

State Key Laboratory of Solid Lubrication, Lanzhou Institute of Chemical Physics, Chinese Academy of Sciences, Lanzhou 730000, PR China

ARTICLE INFO

Article history:
Received 18 December 2010
Received in revised form
28 March 2011
Accepted 29 March 2011
Available online 8 April 2011

Keywords:
TiN
Nanorod
Electrospinning
Electrochemical property
Capacitance

ABSTRACT

TiN nanorods were synthesized using electrospinning technique followed by thermolysis in different atmospheres. A dimethyl formamide–ethanol solution of poly-(vinyl pyrrolidone) and Ti (IV)-isopropoxide was used as the electrospinning precursor solution and as-spun nanofibers were calcined at 500 °C in air to generate TiO_2 nanofibers. Subsequently, a conversion from TiO_2 nanofibers to TiN nanorods was employed by the nitridation treatment at 600∼1400 °C in ammonia atmosphere. A typical characteristic of the final products was that the pristine nanofibers were cut into nanorods. The conversion from TiO_2 to TiN was realized when the nitridation temperature was above 800 °C. As-prepared nanorods were composed of TiN nano-crystallites and the average crystallite size gradually increased with the increase of the nitridation temperature. Electrochemical properties of TiN nanorods showed strong dependence on the nitridation temperature. The maximum value of the specific capacitance was obtained from the TiN nanorods prepared at 800 °C.

1. Introduction

Transition metal nitrides have been studied widely in recent years because of their excellent electrical, mechanical and thermal properties. As a typical transition metal nitride, titanium nitride (TiN) is an important material for many applications because of its superior properties, such as high melting point (2950 °C), high hardness (∼2000 kg/mm^2), high chemical and thermal stability and high electrical and thermal conductivity [1,2]. These attractive properties allow it in many applications such as hard coatings, and the barrier materials in the integrated circuits and heat-conducting films [3–5]. More recently, because of its high electrical conductivity combined with excellent corrosion resistance, TiN has been considered as an excellent candidate for electrode materials in electrochemical capacitors (ECs), which use highly corrosive electrolytes such as potassium hydroxide (KOH), and for electronic conductors in electronic devices [6–9].

Nanostructural materials have exhibited novel physical and chemical properties for the applications in many fields. Up to now, different methods have been employed to synthesize various nanostructural TiN materials, such as chemical vapor deposition [10], sol–gel [11], solid-state metathesis reaction [12] and field-assisted sintering [13]. As a simple and versatile technique, electrospinning can be used for preparing fibers with the diameters ranging from several micrometers to dozens of nanometers [14]. Electrospinning is not only employed in the preparation of polymer nanofibers [15], but is also increasingly applied in inorganic and inorganic composite nanofibers. Recently, various fibrous inorganic metal oxides and non-oxides have been successfully prepared by electrospinning, such as TiO_2 [16], GaN [17], BN [18], ZrN [19] and SiC [20]. So far, electrospinning is not only employed in laboratory research, but is also applied in industry, and it is broadly applicable for sensor, catalysis, filtration, electrode and medicine [21–23].

This paper employed a facile method to prepare TiN nanorods, via a combination of electrospinning and two-step thermolysis. TiO_2 nanofibers were previously prepared from as-electrospun nanofibers by heat-treatment in air and TiN nanorods were obtained by the nitridation treatment of TiO_2 nanofibers at 600∼1400 °C in ammonia atmosphere. The electrochemical properties of as-prepared TiN nanorods exhibited strong dependence on the nitridation temperature. TiN nanorods prepared at 800 °C showed the highest specific capacitance.

2. Experimental

2.1. Materials

Poly-(vinyl pyrrolldone) (PVP, Mw=1,300,000) was purchased from Aladdin Reagent Co., Ltd. Tetra-butyl titanate, $Ti(OC_4H_9)_4$, was purchased from Sinopharm Chemical Reagent Co., Ltd. Ethanol (99.7%) was purchased from Tianjin Rionlon BoHua Medical Chemistry Co., Ltd. Acetic acid and N,N-dimethylfomamide (DMF) were purchased from Tianjin Chemical Reagent Co., Ltd. All reagents were

* Corresponding author. Fax: +86 931 4968055.
E-mail address: xbyan@licp.cas.cn (X. Yan).

0022-4596/$ - see front matter © 2011 Elsevier Inc. All rights reserved.
doi:10.1016/j.jssc.2011.03.053

commercially available and were of analytical reagent grade. Twice-distilled water with a resistance about 18 MΩ cm^{-1} was used throughout.

2.2. Preparation of TiN nanorods

Firstly, 4 g of $Ti(OC_4H_9)_4$ was mixed with 10 ml of ethanol, 8 ml of acetic acid and 4 ml of DMF, and then 1.6 g of PVP was added into the above solution to increase viscidity. Secondly, the mixture was magnetically stirred for 12 h at room temperature (RT) to generate a homogeneous precursor solution. In a typical electrospinning process, the precursor solution was loaded into a plastic syringe equipped with a 23-gage stainless steel needle. A high voltage of 20 kV was supplied by a direct-current power supply and the feeding rate for the precursor solution was adjusted to a constant rate of 0.3 ml/h by a syringe pump. A piece of aluminum foil was placed 15 cm below the tip of the needle to collect the as-spun nanofibers. The process was carried out at RT in air. For the following thermolysis process, as-spun nanofibers were placed in a muffle furnace and calcined at 500 °C in air for 3 h with a heating rate of 1 °C min^{-1} to remove PVP and generate TiO_2 nanofibers. After that, as-prepared TiO_2 nanofibers were heat-treated in a ceramic-tube furnace at different temperatures (600, 800, 1000, 1200 and 1400 °C) in NH_3 gas flow for 5 h with a heating rate of 2 °C min^{-1}.

2.3. Characterization

The morphology and microstructure of the samples were observed using a field emission scanning microscopy (FE-SEM, JSM-6701F) and a transmission electron microscopy (TEM, JEM-2010). The chemical compositions were analyzed by an energy dispersive spectroscopy (EDS) equipped in TEM system. Crystallite structures were determined by a X-ray diffraction (XRD, X′Pert Pro, Philips) using Cu$K\alpha$ radiation from 10° to 80°. Ultraviolet–visible (UV–vis) absorption spectra were obtained from the solid samples dispersed in absolute alcohol, using a Specord 50 UV–visible recording spectrophotometer.

For preparing each working electrode (WE), 80 wt% of TiN sample, 7.5 wt% of acetylene black (> 99.9%), 7.5 wt% of graphite powder and 5.0 wt% of poly (tetrafluoroethylene) were mixed together in an agate mortar until a homogeneous black powder was obtained. The resulting mixture was pressed onto a foam nickel plate (as electric connection) at 10 MPa. The assembled electrode was dried at 80 °C for 16 h in air. Each electrode contained about 4.0 mg of electroactive TiN nanorods and displayed a geometric surface area of about 1 cm^2.

The electrochemical properties of TiN nanorods were investigated using a CHI660D Electrochemical Working Station (ChenHua, China). All measurements were carried out in a conventional glass electrochemistry cell with a three-electrode system in 2 M KOH electrolyte at RT: a WE, a platinum wire counter electrode and a saturated calomel electrode (SCE) reference electrode. The cyclic voltammetry (CV) measurements were conducted with a potential window from −0.8 to 0.2 V at different scan rates ranging from 10 to 200 mV/s. Electrochemical impedance spectroscopy (EIS) measurements were recorded from 10 kHz to 100 MHz with an alternate current amplitude of 5 mV. Galvanostatic charge/discharge measurements were run on from −0.8 to 0.2 V at different current densities, and at open circuit potential. The C was calculated from the slope of each discharge curve, according to the equation $C=(I\,\Delta t)/(\Delta V\,m)$ [24,25], where C is the specific capacitance, I is the constant discharge current, Δt is the discharge time, ΔV is the voltage difference in discharge and m is the mass of the TiN nanorods coated on each WE (4.0 mg in our system).

3. Results and discussion

Fig. 1 shows the SEM images of as-prepared TiO_2 nanofibers and TiN nanorods. TiO_2 nanofibers (Fig. 1a) exhibited ultra-fine fibrous morphology. The lengths reached dozens of micrometers and the average diameter was about 130 nm. In comparison, after the nitridation treatments (Fig. 1b–f), the pristine nanofibers were broken into nanorods with the lengths of several micrometers. Although further shortening in length of nanorods was not found with the increase of the nitridation temperature, the average diameter increased from 135 to 170 nm with increase in temperature from 600 to 1400 °C. It is due to that the TiN grains in nanorods gradually grew with increase in temperature.

Fig. 2a shows a typical TEM image of an individual TiN nanorod synthesized at 1000 °C. This nanorod was composed of crystalline TiN grains. High-resolution TEM image displays fine lattice fringes (Fig. 2b), indicating that good crystallites were

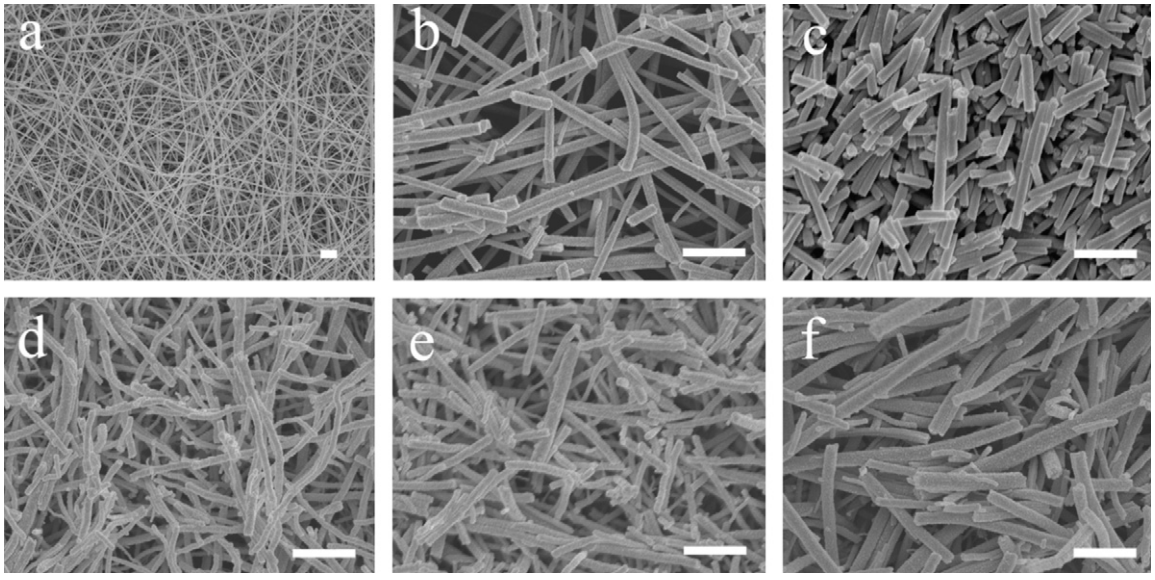

Fig. 1. SEM images of (a) TiO_2 nanofibers and TiN nanorods prepared at different nitridation temperatures: (b) 600 °C, (c) 800 °C, (d) 1000 °C, (e) 1200 °C and (f) 1400 °C. The scales are all 1 μm.

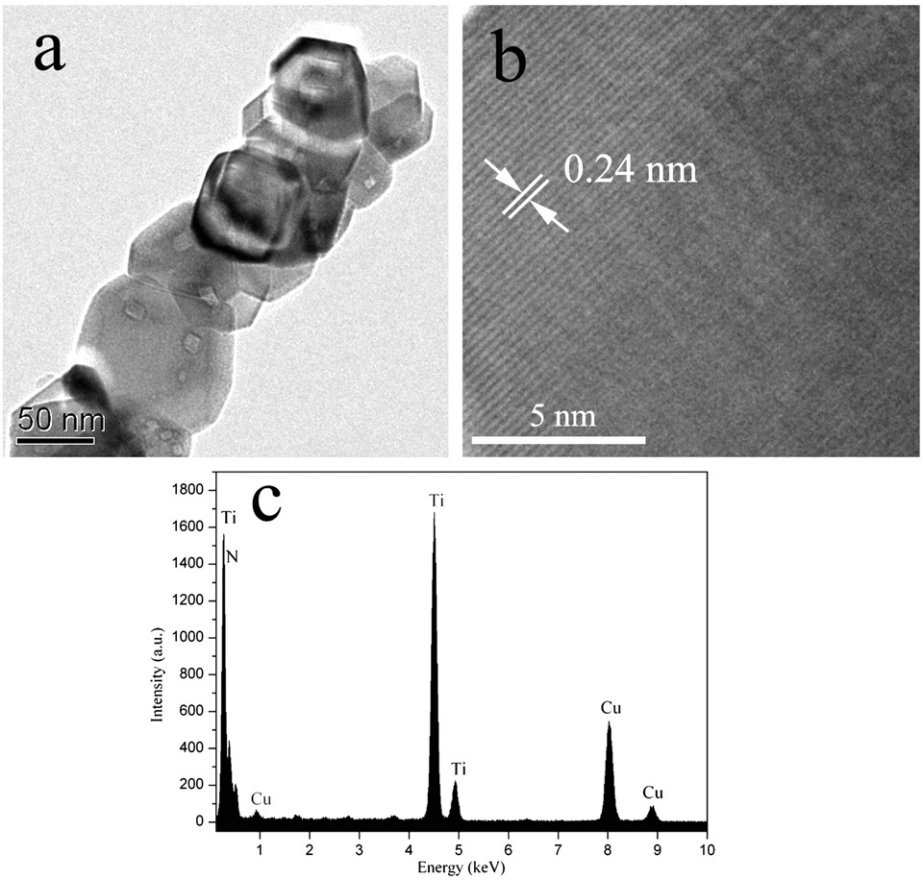

Fig. 2. (a and b) TEM images of an individual TiN nanorod prepared at 1000 °C and its high-resolution image. (c) EDS image of the same sample.

produced without obvious defects. The observed spacing between lattice fringes was measured to be 0.24 nm,corresponding to the (1 1 1) plane of TiN. The elemental analysis of TiN nanorods prepared at 1000 °C was done using EDS. As shown in Fig. 2c, obvious signals attributed to Ti and N appeared, indicating the sample consisted of Ti and N atoms. Lack of O signal indicated the entire conversion from TiO_2 to TiN. It should be mentioned that the signal attributed to Cu atom came from the copper grid for TEM testing.

In order to investigate the effect of nitridation temperature on the crystalline structure, as-prepared TiO_2 nanofibers and TiN nanorods were characterized by XRD. As shown in Fig. 3, XRD pattern (a) indicates the formation of pure anatase TiO_2 phase through the calcination at 500 °C in air. Compared with TiO_2 nanofibers, XRD pattern (b) displays the characteristic diffraction peaks, assigned to TiN phase at 36.90°, 43.30° and 62.52°, respectively, indicating that cubic-phase TiN began to be formed at 600 °C. In addition, the characteristic TiO_2 peaks at 25.25°, 47.76° and 54.61° still were remained, indicating an incomplete nitridation at this temperature. As shown in XRD patterns (c–f), pure TiN phase was generated when the nitridation temperature was above 800 °C. In these patterns, the diffraction peaks ($36.85 \pm 0.3°$, $42.78 \pm 0.3°$, $61.96 \pm 0.3°$, $74.51 \pm 0.3°$ and $78.02 \pm 0.3°$) matched well with the (111), (200), (220), (311) and (222) reflections of cubic TiN, respectively. Zukalova et al. [26] obtained the relatively pure TiN ($TiO_{0.004}N_{0.96}$) by the nitridation treatment at 1000 °C and its lattice constant was 4.229 Å. They believed that the existence of oxygen composition resulted in the decrease of the lattice constant compared with that of pure TiN phase. In our synthesis, the lattice constants of TiN (800, 1000, 1200 and 1400 °C) calculated from the XRD patterns were 4.213, 4,225, 4.241 and 4.246 Å, respectively.

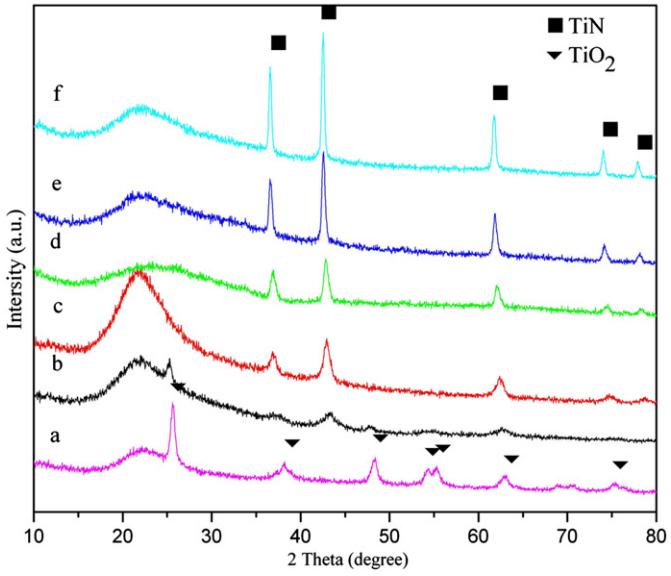

Fig. 3. XRD patterns of (a) TiO_2 nanofibers and TiN nanorods prepared at different nitridation temperatures: (b) 600 °C, (c) 800 °C, (d) 1000 °C, (e) 1200 °C and (f) 1400 °C.

The lattice constants of the samples prepared at 1000, 1200 and 1400 °C were nearly equal to or larger than the value of 4.229 Å, indicating that these samples were pure TiN. It should be mentioned that the lattice constant of the sample prepared at 800 °C was smaller than the value of 4.229 Å, which indicated that this sample contained small quantity of oxygen composition. Also, these

diffraction peaks became sharper and narrower with the increase of nitridation temperature, suggesting better crystallinity at higher temperature. Additionally, these peaks moved slightly to the lower angle direction with increase in temperature, suggesting the decrease of oxygen content with elevated nitridation temperature [26]. The average crystallite sizes of TiN nanorods prepared at different temperatures, calculated by the Scherrer equation, were 4.9 nm for 600 °C, 12 nm for 800 °C, 17 nm for 1000 °C, 23 nm for 1200 °C and 28 nm for 1400 °C.

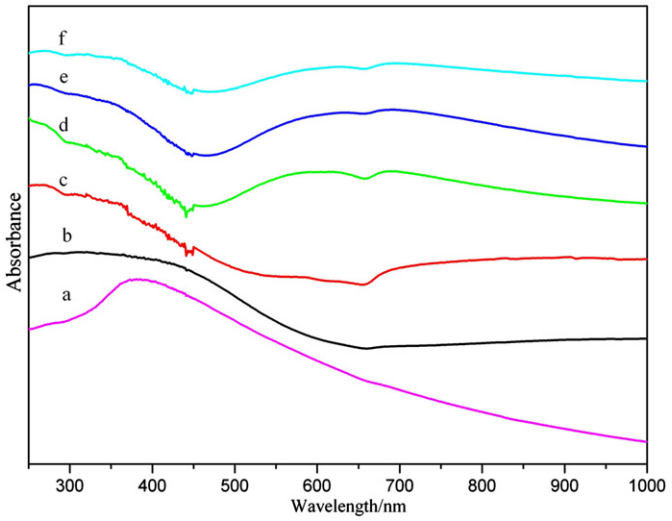

Fig. 4. UV–vis adsorption spectra of (a) TiO_2 nanofibers and TiN nanorods prepared at different nitridation temperatures: (b) 600 °C, (c) 800 °C, (d) 1000 °C, (e) 1200 °C and (f) 1400 °C.

To further study such structural change, UV–vis spectra of the samples were also measured. As shown in Fig. 4a, for pure TiO_2 nanofibers, an obvious absorption peak centered at 380 nm was assigned to the intrinsic band gap absorption of anatase TiO_2 and there was no obvious absorption in the visible region. In comparison, for the TiN nanorods prepared at 600 °C (Fig. 4b), the absorption intensity at 380 nm decreased owing to the started transition from anatase TiO_2 to TiN. When the nitridation temperature was above 800 °C, the absorptions (Fig. 4c–f) became stronger in the visible range compared with those shown in Fig. 4a and b. Additionally, a broad absorption band ranging from 480 to 900 nm was observed in Fig. 4d–f. The appearance of this peak was related to the formation of TiN crystallites and the up-shifting of the central position was also related to the TiN crystallite size.

In our experiments, when as-spun PVP-precursor composite nanofibers were pyrolyzed in air, PVP and organic compounds in Ti $(OC_4H_9)_4$ were burned out, as a result of the formation of inorganic TiO_2. Afterwards, the inorganic TiO_2 crystallized into anatase TiO_2 during the calcination at 500 °C. It is known that metal oxides can be converted into metal nitrides by hot NH_3 gas when the heating temperature is high enough. Therefore, in our experiments, when the nitridation temperature was above 600 °C, anatase TiO_2 in TiO_2 nanofibers would react with NH_3 to form TiN. Especially, when the temperature was ranging from

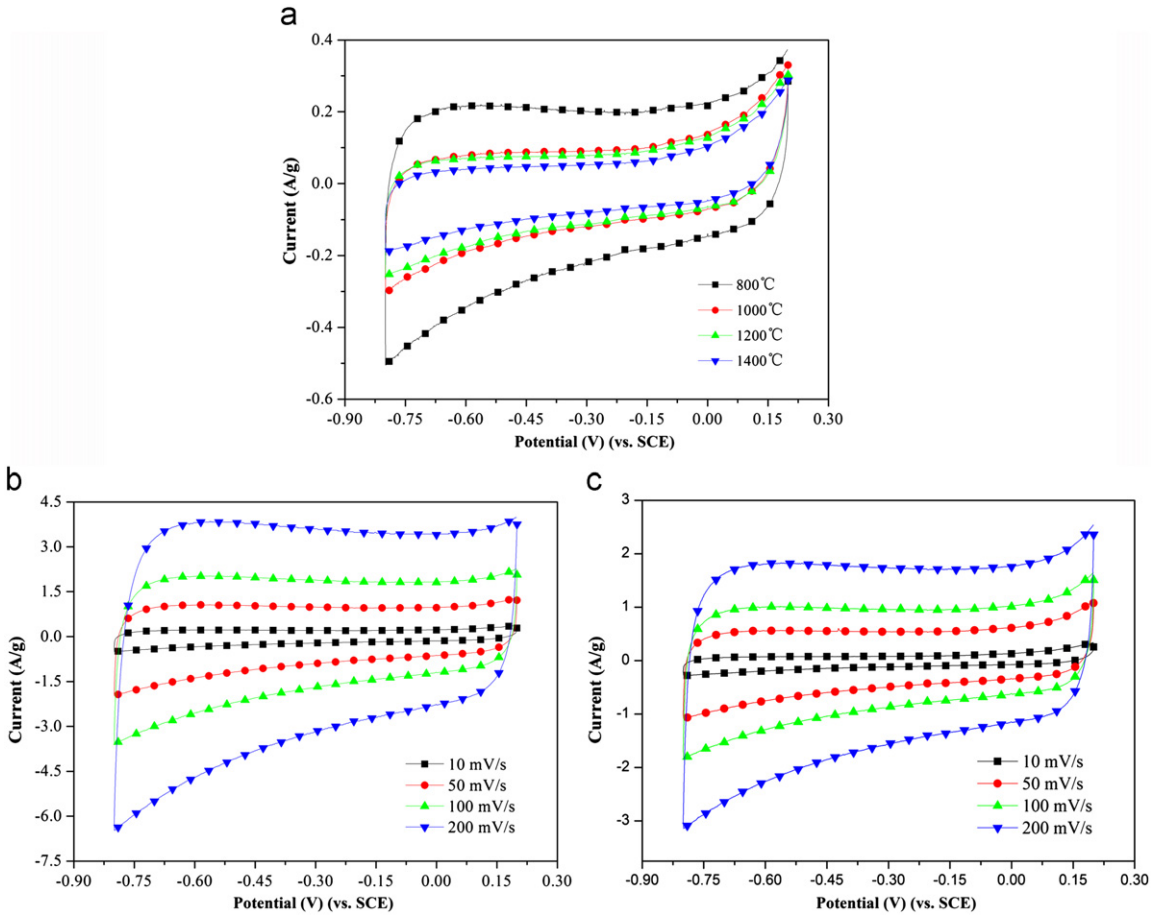

Fig. 5. (a) CV curves of TiN nanorods prepared at different nitridation temperatures scanned at a scan rate of 2 mV/s. (b) CV curves of TiN nanorods prepared at 800 °C scanned at different scan rates. (c) CV curves of TiN nanorods prepared at 1200 °C scanned at different scan rates.

800 to 1400 °C, a conversion from TiO_2 to TiN could be finished. Furthermore, it is known that TiO_2 nanofibers prepared by electrospinning are composed of TiO_2 nanoparticles [16], which directionally accumulate to form fibrous structure. Such particle-accumulated fibers have a large quantity of defects and pores. In some areas, the density of defects and pores is relatively high. Therefore, we assume that, in our experiments, the nitridation reaction of TiO_2 occurred on these areas would result in the breaking of the pristine fibrous structure. Finally, TiN nanorods were obtained.

The electrochemical properties of the TiN nanorods were studied by CV, galvanostatic charge/discharge and EIS. Fig. 5a shows the CV curves of different TiN electrodes taken between −0.8 and 0.2 V at a scan rate of 10 mV/s. All CV curves exhibited ideal rectangular shapes, indicating that the capacitance characteristic of the TiN phase was the electric double-layer capacitance. Moreover, the current density response and the CV curve area both decreased with the increase of the nitridation temperature, especially from 800 to 1000 °C. In order to further examine the electrochemical performance of the TiN nanorods, the TiN nanorods containing small oxygen (800 °C) and pure TiN nanorods (prepared at 1200 °C) were discussed, and its CV curves scanned at different scan rates (10∼200 mV/s) are shown in Fig. 5b and c. With the increase of the voltage sweep rate, the curves preserved the rectangular shape, indicating the typical electric double-layer capacitive behavior. Also, the current density response gradually increased with increase in the scan rate. The CV area of the sample prepared at 1200 °C was smaller than that of the sample prepared at 800 °C at the same scan rate.

Fig. 6a shows the galvanostatic charge/discharge curves of different TiN electrodes, obtained at a constant current density of 40 mA/g. It is obviously seen that the charge/discharge times were prolonged with the decrease of the nitridation temperature from 1400 to 800 °C. It indicates that the specific capacitance was inversely proportional to the nitridation temperature. According to the capacitance equation evaluated from the slopes of the discharge curves (shown in the Section 2), the specific capacitance of TiN nanorods prepared at different temperatures (800, 1000, 1200 and 1400 °C) was about 38.5, 20.2, 17.0 and 11.5 F/g, respectively. Therefore, the TiN nanorods prepared at 800 °C had the highest specific capacitance. We believe that the decrease in the capacitance was mainly attributed to the decreased active surface area of TiN crystallites, which resulted from the increased crystallite size with increase in temperature. Jiang and Guo [6] reported that the specific capacitance of TiN nanoparticle prepared by ammonia nitridation at 800 °C was 11.53 F/g. The relatively high specific capacitance in our system was probably due to the one-dimensional nanorod-like structure. Fig. 6b and c displays the dependence of the specific capacitance of the TiN nanorods (prepared at 800 and 1200 °C) on the current density in the range of 40∼640 mA/g^{-1}. It is clearly seen that the specific capacitance gradually decreased with the increase of discharge current density. It indicates that the TiN electrode allowed rapid ion diffusion, and the specific capacitance of the sample prepared at 1200 °C was lower than that of the sample prepared at 800 °C at the same discharge current density. Fig. 7 further reveals that the value of the specific capacitance was strongly dependent on the nitridation temperature and the employed current density.

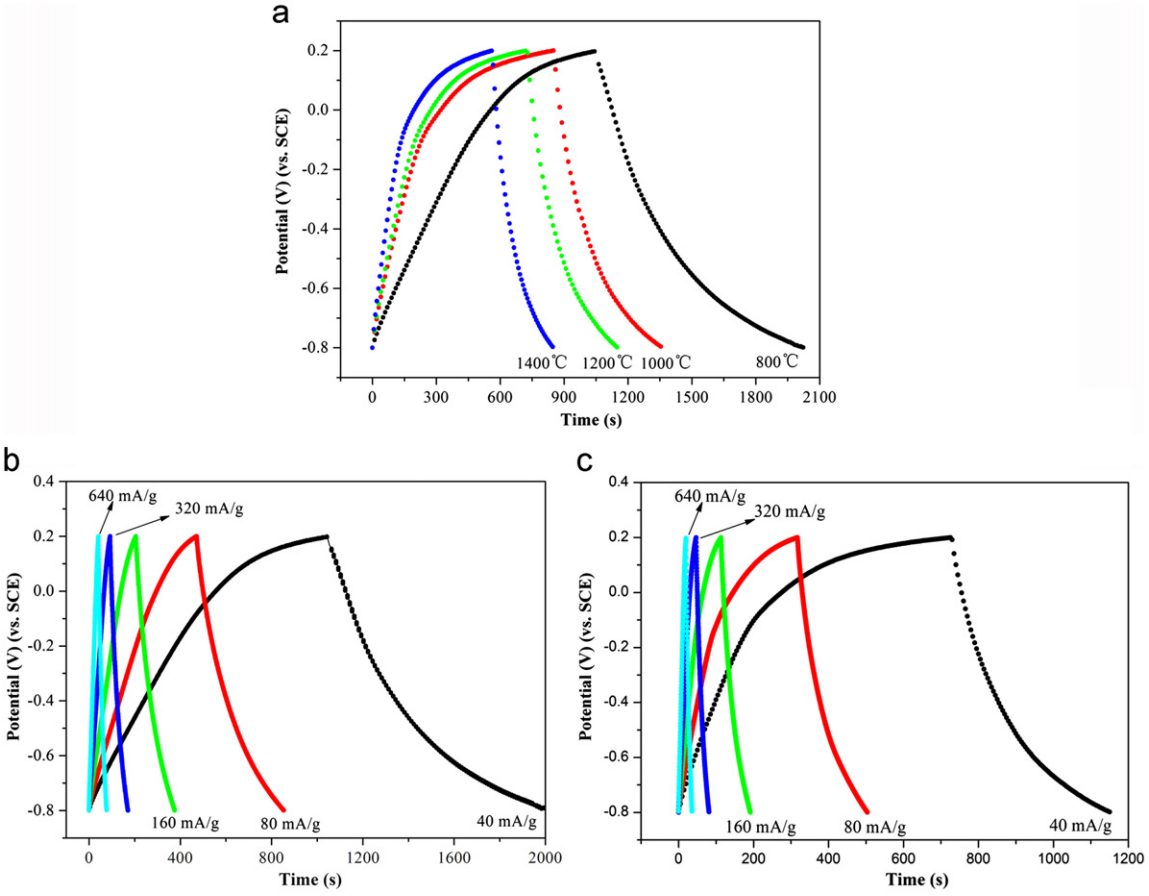

Fig. 6. (a) Galvanostatic charge–discharge curves of TiN nanorods prepared at different nitridation temperatures at a current density of 40 mA/g. (b) Galvanostatic charge–discharge curves of TiN nanorods prepared at 800 °C at different current densities. (c) Galvanostatic charge–discharge curves of TiN nanorods prepared at 1200 °C at different current densities.

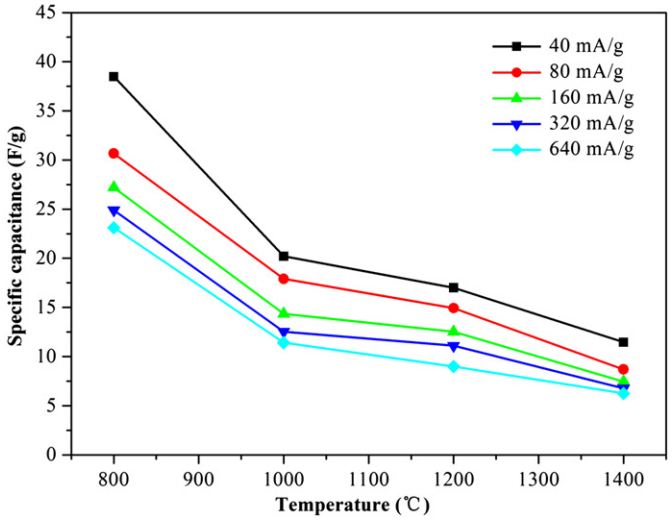

Fig. 7. The specific capacitance as the function of the nitridation temperature and the current density.

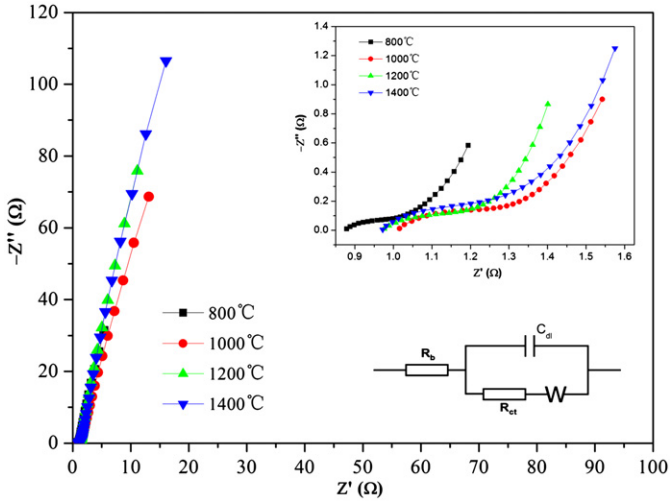

Fig. 8. Nyquist plot of TiN nanorods prepared at different temperatures. Inset in the upper right corner is the enlarged plots of the high-frequency regions. Inset in the lower right corner is the equivalent circuit.

Specifically, it would decrease with the increase of the nitridation temperature or with the increase of the current density.

EIS is used to investigate the performance of electrochemical capacitors such as internal resistance, capacity, etc [27]. The EIS data are analyzed using Nyquist plots, which show the frequency response of the electrode/electrolyte system and are the plots of the imaginary component (Z″) of the impedance against the real component (Z′). Fig. 8 shows the relation between Z″ and Z′ impedance components of TiN nanorods prepared at different temperatures. The complex-plane impedance plots for each sample could be divided into the high-frequency component and the low-frequency component. A distinct knee in the frequency was observed in the inset of Fig. 8. From the point intersecting with the real axis in the range of high frequency, the internal resistances (which is equal to *Rb*) of the TiN electrodes were 0.88, 1.02, 0.98 and 0.97, corresponding to the TiN nanorods obtained at 800, 1000, 1200 and 1400 °C, respectively. The value includes the total resistances of the ionic resistance of electrolyte, intrinsic resistance of active materials and contact resistance at the active material/current collector interface. The semicircle in the high-frequency range associated with the surface properties of electrode corresponds to the faradic charge-transfer resistance (*Rct*). In our system, the TiN nanorods obtained at 800 °C showed the smallest internal resistances, and the value of *Rb* decreased with the increase of the nitridation temperature. Moreover, all TiN nanorods had small charge-transfer resistance. At low frequencies, a straight slope line represents the diffusive resistance (Warburg impendence) of the electrolyte in electrode pores and the proton diffusion in host material [27]. The phase angles for impedance plots of all TiN nanorod electrodes were observed to be higher than 45° in the low frequencies. These findings suggest that all the electrodes were not strongly controlled by diffusion process, implying the good accessibility of the ions and/or the possible contributions of electrochemical capacitors [28].

4. Conclusions

In summary, we demonstrated the preparation of TiN nanorods via combined electrospinning and thermolysis. TiO_2 nanofibers, generated in the first-step thermolysis process, were converted into TiN nanorods through the second-step high-temperature nitridation process. Relatively pure TiN nanorods were generated when the nitridation temperature was above 800 °C. This synthetic strategy can be extended to the preparation of other nanorod-like metal nitrides. Moreover, the electrochemical capacitances of as-prepared TiN nanorods showed strong dependence on the nitridation temperatures and the TiN nanorods obtained at 800 °C displayed the highest specific capacitance.

Acknowledgments

This work was supported by the Top Hundred Talents Program of Chinese Academy of Sciences, the National Basic Research 973 Program of China (2011CB706603) and the National Nature Science Foundation of China (51005225).

References

[1] J.Q. Hu, Q.Y. Lu, K.B. Tang, et al., J. Am. Ceram. Soc. 83 (2000) 430.
[2] J.H. Ma, M.N. Wu, Y.H. Du, et al., J, Alloys Compd. 476 (2009) 603.
[3] E. Velkonen, T. Karlsson, B. Karlsson, et al., Proc. SPIE 401 (1983) 41.
[4] P.J. Ireland, Thin Solid Films 304 (1997) 1.
[5] R. Buhl, H.K. Pulker, E. Moll, Thin Solid Films 80 (1981) 265.
[6] L.Q. Jiang, L. Guo, J. Am. Ceram. Soc. 89 (2006) 156.
[7] C.F. Hsieh, S. Jou., Microelectr. J. 37 (2006) 867.
[8] Q.W. Jiang, G.R. Li, X.P. Gao, Chem. Commun. (2009) 6720.
[9] D. Choi, P.N. Kumta, J. Electrochem. Soc. 153 (2006) A2298.
[10] N. Ramanuja, R.A. Levy, S.N. Dharmadhikari, et al., Mater. Lett. 57 (2002) 261.
[11] K. Kamiya, T. Yoko, M. Bessho, J. Mater. Sci. 22 (1987) 937.
[12] U.A. Joshi, S.H. Chung, J. Sung, J. Solid State Chem. 178 (2005) 755.
[13] J.R. Groza, J.D. Curtis, M. Kramer, J. Am. Ceram. Soc. 83 (2000) 1281.
[14] M. Bognitzki, W. Czado, T. Frese, et al., Adv. Mater. 13 (2001) 70.
[15] D.H. Reneker, I. Chun, Nanotechnonlogy 7 (1996) 216.
[16] D. Li, Y.L. Wang, Y.N. Xia, Nano Lett. 3 (2003) 1167.
[17] H. Wu, Y. Sun, D.D. Lin, et al., Adv. Mater. 20 (2008) 1.
[18] Y.J. Qiu, J. Yu, J. Rafique, et al., J. Phys. Chem. C 113 (2009) 11228.
[19] J.Y. Li, Y. Sun, Y. Tan, et al., Chem. Eng. J. 144 (2008) 149.
[20] D.G. Shin, D.H. Riu, H.E. Kim, J. Ceram. Process. Res. **9** (2008) 209.
[21] A. Greiner, J.H. Wendorff, Angew. Chem. Int. Ed. 46 (2007) 5670.
[22] P.W. Gibson, H.L. Schreuder-Gibson, D. Rivin, AIChE J. 45 (1999) 190.
[23] L. Huang, R.A. McMillan, R.P. Apkarian, et al., Macromolecules 33 (2000) 2989.
[24] W. Xing, X. Yuan, S.P. Zhuo, et al., Adv. Technol. 20 (2009) 1179.
[25] C. Kim, J. Power Sources 142 (2005) 382.
[26] M. Zukalova, J. Prochazka, Z. Bastl, et al., Chem. Mater. 22 (2010) 4045.
[27] G.H. Sun, K.X. Li, C.G. Sun., Micropor. Mesopor. Mater. 128 (2010) 56–61.
[28] M.D. Stoller, S. Park, Y.W. Zhu, et al., Nano Lett. 8 (2008) 3498.